UC-94c
LBL-20990
Preprint

Lawrence Berkeley Laboratory
UNIVERSITY OF CALIFORNIA

LAWRENCE
BERKELEY LABORATORY
MAR 20 1986
LIBRARY AND
DOCUMENTS SECTION

APPLIED SCIENCE DIVISION

Submitted to Journal of the Electrochemical Society

KINETICS OF AQUEOUS POLYSULFIDE SOLUTIONS: PART II. ELECTROCHEMICAL MEASUREMENT OF THE RATES OF COUPLED ELECTROCHEMICAL AND CHEMICAL REACTIONS BY THE POTENTIAL STEP METHOD

P. Lessner, J. Winnick, F.R. McLarnon,
and E.J. Cairns

January 1986

For Reference
Not to be taken from this room

APPLIED SCIENCE
DIVISION

LBL-20990
c.1

Prepared for the U.S. Department of Energy under Contract DE-AC03-76SF00098

DISCLAIMER

This document was prepared as an account of work sponsored by the United States Government. While this document is believed to contain correct information, neither the United States Government nor any agency thereof, nor the Regents of the University of California, nor any of their employees, makes any warranty, express or implied, or assumes any legal responsibility for the accuracy, completeness, or usefulness of any information, apparatus, product, or process disclosed, or represents that its use would not infringe privately owned rights. Reference herein to any specific commercial product, process, or service by its trade name, trademark, manufacturer, or otherwise, does not necessarily constitute or imply its endorsement, recommendation, or favoring by the United States Government or any agency thereof, or the Regents of the University of California. The views and opinions of authors expressed herein do not necessarily state or reflect those of the United States Government or any agency thereof or the Regents of the University of California.

LBL-20990
Preprint

KINETICS OF AQUEOUS POLYSULFIDE SOLUTIONS: PART II. ELECTROCHEMICAL MEASUREMENT OF THE RATES OF COUPLED ELECTROCHEMICAL AND CHEMICAL REACTIONS BY THE POTENTIAL STEP METHOD

P. Lessner, J. Winnick,† F.R. McLarnon and E.J. Cairns

Applied Science Division
Lawrence Berkeley Laboratory, and
Department of Chemical Engineering
University of California
Berkeley, California 94720

January 1986

* This work was supported by the Assistant Secretary for Conservation and Renewable Energy, Office of Energy Storage and Distribution of the U.S. Department of Energy under Contract No. DE-AC03-76SF00098.

† Present address: Georgia Institute of Technology, Department of Chemical Engineering, Atlanta, Georgia 30332

Kinetics of Aqueous Polysulfide Solutions: Part II. Electrochemical Measurement of the Rates of Coupled Electrochemical and Chemical Reactions by the Potential Step Method

Philip Lessner, Jack Winnick,* Frank R. McLarnon
and
Elton J. Cairns

Applied Science Division
Lawrence Berkeley Laboratory
and
Department of Chemical Engineering
University of California
Berkeley, CA 94720

January 1986

Abstract

The kinetics of the aqueous polysulfide redox couple were investigated using a potential step technique in a 1 M Na_2S_4 solution at pH 12. The low overpotential region (-20 to +20 mV) on cobalt and platinum electrodes was investigated from 25 to 80 C. The active species concentration was found to be several orders of magnitude lower than those of any of the major (poly)sulfide ions, and its temperature dependence corresponded to an E_a of about 10 kcal/mole. These results are consistent with the active species being S_2^-. Deviations were found at temperatures above 45 C between experimental data and the simple analytical form for the current response for an electrode reaction with one rate-determining step. The results agree with a new model that considers two rate-determining steps, one of which is the reaction $S_4^{2-} \rightleftarrows 2S_2^-$. The rate constants for this reaction determined using this new model agree with those measured for similar reactions.

*Present Address: Georgia Institute of Technology, Department of Chemical Engineering, Atlanta, Georgia 30332

Introduction

Recently there has been renewed interest in the electrochemistry of the aqueous polysulfide redox couple because of its potential application in energy conversion and storage devices such as photoelectrochemical cells and redox batteries (1-3). This couple is attractive because it meets several practical requirements for photoelectrochemical cells: it stabilizes $CdSe_xTe_{1-x}$ systems with band gaps around 1.45 eV, sulfur and sodium sulfide are soluble in molar concentrations, and the electrolyte is relatively low in cost. Despite the increasingly widespread interest in this couple, little of a quantitative nature is known about its solution electrochemistry in the low overpotential range. It is in this range that both the semiconductor and redox electrodes must operate if an efficient energy-conversion or storage device is to be practical.

Two major problems with aqueous polysulfide-based photoelectrochemical cells are efficiency and long-term stability. Stability refers to photocorrosion: the tendency of the semiconductor photoanode to oxidize itself instead of the reduced species in solution. Two approaches to improving the efficiency and stability of a photoelectrochemical cell are to make modifications to the photoelectrode and counterelectrode, or to modify the composition of the electrolyte. Both approaches have been used successfully in the polysulfide system. Differences in preparation techniques (4), etching (5), and photoetching (2) of the photoelectrode lead to marked differences in cell output. Selection of the proper electrocatalyst for the counterelectrode can lead to reduced overpotential and therefore increased cell voltage (6). Modification of the solution composition by changing the sulfur to sulfide ratio (7), pH (8) and cation (9) have all led to stability and/or efficiency improvements.

It is difficult to obtain fundamental data on the electrochemistry of the polysulfide couple at semiconductor electrodes because the current-voltage characteristics are dominated by processes internal to the semiconductor, and therefore surface-solution overpotentials are difficult to measure. The investigations on dark electrocatalysts, which began in 1928 with Fetzer (10), do not provide all of the information needed to rationally improve the solution composition. Investigations have been carried out either in solutions with compositions far from what

is used in practical photoelectrochemical cells (11,12), were semiquantitative in nature (6) or were carried out in the Tafel region (13).

In this work we use a potential step method to obtain information about aqueous polysulfide electrochemistry. This technique was selected because it offers the possibility of determining both the exchange current density and the electroactive species concentration. The applicability of this method in the linear overpotential region has been well analyzed (14,15). It is anticipated that the information we have obtained can be used to make rational modifications to the polysulfide solution composition in order to improve the kinetics on both the photoelectrode and the counterelectrode.

Selection of Electrolyte Composition and Electrocatalyst

Schwarzenbach and Fischer (16) used chemical methods to show that S_4^{2-} (tetrasulfide), was the major species present in aqueous polysulfide solutions. Teder used both chemical (17) and spectroscopic (18,19) methods to determine sulfur solubility and polysulfide distribution. These spectroscopic investigations were extended by Giggenbach who derived a set of equilibrium constants for equilibria among the polysulfide ions (20). In addition to polysulfide ions, both monosulfide species and sulfur radicals are present. Giggenbach (21) proposed that the major sulfur radical present is S_2^- (supersulfide), and he studied the equilibria between tetrasulfide and supersulfide as a function of temperature. There has been much controversy concerning the second acidity constant of hydrogen sulfide (22). Giggenbach (23) used an ultraviolet spectroscopic technique to derive a value that was considerably smaller than any previously reported. This value has recently been confirmed by Meyer using a raman spectroscopic technique (24).

Table I shows the sulfide, polysulfide and sulfur radical species present in a 1 M polysulfide solution at pH 12, as a function of temperature. The average polysulfide chain length under these conditions is very close to 4. These concentrations were calculated by using the equilibrium constants given by Giggenbach (20,21), and the major species in solution are S_4^{2-} and HS^-. These equilibrium constants were calculated from observations on dilute (less than 0.1 M) solutions of polysulfides. The equilibrium constants are not corrected for the (unknown) activities of the

polysulfide ions. In the more concentrated solutions employed here some deviation between the calculated and actual species concentrations might be expected. The distribution of the polysulfide ions does not vary appreciably with temperature (25), although equilibria between bisulfide and sulfide shows some dependence on temperature (23). The concentration of supersulfide is strongly dependent on the temperature (21).

Polysulfides can be converted into sulfur oxyanions by three principal methods: exposure to oxygen, electrochemical oxidation and homogeneous disproportionation. Exposure to air can be minimized by operating a sealed cell or passing an inert gas over the electrolyte. Both Gerischer (11), and Allen and Hickling (13) showed that no appreciable oxidation of polysulfides to sulfur oxyanions took place at anodic overpotentials of less than 200 mV. Giggenbach (25,26) has shown that polysulfide solutions spontaneously disproportionate to thiosulfate. Recent data show that this reaction can have an effect on the efficiency of photoelectrochemical cell operation (27).

Higher polysulfides are converted into thiosulfate via reactions such as:

$$S_5^{2-} + 3OH^- \rightleftarrows S_2O_3^{2-} + 3HS^- \qquad (1)$$

Both the equilibrium constants and rates of Reaction 1 have been measured (25,26). The equilibrium amount of thiosulfate is dependent on temperature, pH, and sulfur to sulfide ratio. It increases as temperature and sulfur to sulfide ratio increase. At low pH, where S_5^{2-} and S_4^{2-} are the major species, the thiosulfate concentration increases with increasing pH. At very high pH, the concentration of thiosulfate decreases because the lower polysulfide ions S_3^{2-} and S_2^{2-}, which are stable, are the dominant species.

The forward rate of Reaction 1 is slow at room temperature, but it increases significantly as the temperature is raised (26). A compromise is necessary in selecting a solution composition because the factors that produce optimum kinetics in a fresh polysulfide solution may also lead to accelerated degradation. For example, increasing the sulfur to sulfide ratio is known to decrease overpotential, but from Reaction 1 it is seen to increase the equilibrium amount and rate of conversion to thiosulfate. We chose a pH of 12 for our investigations because calculations using published data (26) showed that it would take several days even at elevated temperatures to con-

vert 1% of the polysulfide to thiosulfate.

Several criteria determined the choice of an electrocatalyst for this study. The electrocatalyst should exhibit exchange current densities that are sufficiently large to suggest its use as a practical counterelectrode for a photoelectrochemical cell, it should be capable of being polished to a reproducible surface area, and it should not significantly change its properties upon long-term exposure to polysulfide electrolyte. Several electrocatalysts were evaluated in preliminary experiments, and Table II shows the results of those experiments. Cobalt was chosen as the electrocatalyst to be used in most of these studies, and platinum was used for comparison purposes.

Experimental Procedure

Figure 1 shows a block diagram of the experimental apparatus. A PAR model 175 function generator was used to apply potential pulses to a PAR model 371 potentiostat/galvanostat which controlled a three-electrode cell. Potentials could be set with a precision of about ±0.1 mV. The cell current was monitored via a resistor placed between the counterelectrode and the potentiostat. Transient current responses were stored on a Nicolet digital oscilloscope which at its maximum rate allows data to be recorded at 500 ns intervals. Current-time pairs could then be read directly from the screen via a cursor. Typically 15-30 points were read for each transient. The potentiostat/galvanostat was operated in galvanostatic mode in order to obtain double-layer capacity data and the ohmic potential drop in solution using the current step method.

A diagram of the cell used in these experiments is shown in Figure 2. The body of the cell is a 1/2 inch nylon tube cross. For operation at temperatures higher than ambient, a thermocouple was placed against the cell body, and the cell was wrapped in heating tape, asbestos pipe tape, and high-temperature furnace insulation. The temperature could be controlled within 0.2 °C for several hours by setting the power input to the heating tape. The working (0.2 cm^2 Co and 0.32 cm^2 Pt) and counterelectrode disks were mounted in nylon rods, and the reference electrode was a platinum wire. The working electrode was placed in the center of the channel in order to minimize the ohmic drop between it and the reference electrode, and the electrodes were attached to the cell via ferrules to assure a leak-tight fit. Provisions were made to introduce the electrolyte under

a vacuum, and the cell was sealed to minimize contact of the polysulfide electrolyte with air.

The electrolyte was prepared by adding weighed amounts of 99.999% sulfur and $Na_2S \bullet 9H_2O$ (reagent-grade) to water (deionized, with resistivity greater than 1.2 MΩ-cm) which had been deoxygenated for at least one hour by bubbling nitrogen or argon through it. Hydrogen sulfide (Matheson, C.P. grade, 99.5%) was bubbled through the electrolyte to adjust the pH and sulfur to sulfide ratio to the desired values. The electrolyte was then quickly transferred to a volumetric flask fitted with a rubber septum. A slight vacuum was applied to degas the solution and fill any air space in the flask with argon. When an experiment was performed the flask was slightly pressurized, and the electrolyte was transferred via a syringe.

The amount of zero-valent sulfur added to the electrolyte could be controlled accurately by weighing the solid sulfur on an analytical balance (precise to 0.1 mg), but there was a greater uncertainty in the concentration of sulfide present. A sample of solution was analyzed for total sulfur by oxidation to sulfate using alkaline hydrogen peroxide, and precipitation of barium sulfate with barium chloride. The concentration of zero-valent sulfur was then subtracted from the total sulfur to determine the concentration of sulfide.

Electrical contact to the working electrode and the counterelectrode was made via stainless steel rods and silver epoxy. To protect this junction from the aggressive polysulfide electrolyte a piece of heat shrinkable PTFE tubing was placed around the electrode disk, and silicone sealant was used to seal the assembly into the nylon holder. This arrangement remained leak free as the temperature of the system was changed.

The mounted electrodes were polished with a succession of silicon carbide and emery abrasives, and final polishing was done with one-micron diamond paste. The electrodes were rinsed with acetone and distilled water before use.

Results

Experiments were performed over the temperature range of 25 - 80 C. After introduction of the electrolyte, several minutes were required for the reference and working electrodes to reach

the same potential. A potential step was applied only after the potentials differed from each other by no more than 2 mV. The platinum reference electrode was checked against an SCE, and its potential was found to be that of the polysulfide redox couple. The double-layer capacitance and ohmic resistance were measured, and data were taken only at times greater than $4R_sC_{dl}$, where capacitive current is expected to contribute less than 1% to the total current. Some typical cathodic transients are shown in Figure 3, where the points are experimental data and the lines represent fits to Equation 2 as discussed below. Both anodic and cathodic steps were applied; the anodic currents were 10-20% higher at the same overpotential and the anodic curves had a slightly flatter shape.

An attempt was made to fit each current transient to Nagy's equation (15):

$$i = (W/t_2\lambda^2)[\exp(\lambda^2 t)\mathrm{erfc}(\lambda t^{1/2}) + 2\lambda(t/\pi)^{1/2} - \exp(\lambda^2(t-t_2))\mathrm{erfc}(\lambda(t-t_2)^{1/2}) - 2\lambda((t-t_2)/\pi)^{1/2}] \qquad (2)$$

where

$$W = \frac{V}{R_s+R_r} \qquad (3)$$

$$\lambda = \frac{i_o}{\nu nF} \cdot \frac{R_r}{R_s+R_r}\left(\frac{1}{D_o^{1/2}C_{ob}} + \frac{1}{D_r^{1/2}C_{rb}}\right) \qquad (4)$$

Several assumptions go into the derivation of Equation 2. Briefly they are: a well-supported electrolyte, one overall electrode reaction ($O + ne^- \rightleftarrows R$) with one rate-determining step, linear kinetics, no diffusion of intermediates away from the electrode and no strong specific adsorption.

At temperatures below 45 C a good fit could be obtained between the experimental data and Equation 2 in the time range of 0.5 to 10 ms. A reproducible value of the diffusion parameter $1/D_o^{1/2}C_{ob}+1/D_r^{1/2}C_{rb}$ was obtained from all data sets, and at each temperature, but the values of λ and W were sensitive to the value chosen for t_2, the rise time of potential across the double layer, at lower temperatures. A check of the applicability diagrams published by Nagy (15) showed that the system was near to the edge of the applicability field at the lower temperatures.

At higher temperatures, the response curves became flatter suggesting an increase in electroactive species concentration. The fit to the short-time data (less than 2 ms) was good, but the model consistently underestimated the currents at later times. Possible reasons for this are

suggested in the discussion section.

The points in Figure 4 show the active species concentration evaluated[1] from the lower-temperature data and the fit to the short-time data at higher temperatures. The active species concentration is seen to be lower than any of the major poly or monosulfide species, and it increases with temperature with an apparent activation energy of about 10 kcal/mole.

Slow-sweep voltammetry was attempted in order to obtain kinetic and diffusion information. Observation of meaningful peaks was obscured by side reactions in both the anodic and cathodic directions. At the anodic diffusion peak sulfur was deposited, and hydrogen was usually evolved on cathodic scan before a well-defined diffusion peak could be observed. Some potential step measurements were performed on platinum; the shapes of the transients were similar to those on cobalt, but the current densities were much lower. Fast potential sweep experiments (10 - 100 V/sec) were also performed; the derived reaction resistances were of the same order of magnitude as those obtained from the fits to the potential step data.

Discussion

The overall electrode reaction in polysulfide solutions can be written in a number of equivalent ways. In tables of electrode potentials it is usually written (30):

$$S + 2e^- \rightleftarrows S^{2-} \tag{5}$$

while others (13,31) have suggested a form similar to:

$$S_2^{2-} + 2H_2O + 2e^- \rightleftarrows 2HS^- + 2OH^- \tag{6}$$

In the polysulfide solutions used here S_4^{2-} and HS^- are the dominant species suggesting that the overall reaction can be written as:

$$1/3S_4^{2-} + 4/3H_2O + 2e^- \rightleftarrows 4/3HS^- + 4/3OH^- \tag{7}$$

However, it is apparent from Figure 4 that the calculated active species concentration is several orders of magnitude lower than that of any of the species participating in Reaction 7. This leads

[1] To obtain the active species concentration from the diffusion parameter two assumptions were needed. First, the diffusion coefficients were assumed to be equal. Their values were assumed to be close to $10^{-5}cm^2/sec$ at room temperature (28), and a correction was applied at elevated temperatures (29). Second, the value of C_{rb} was assumed to be much greater than C_{ob}. This is justified in the discussion below.

to the conclusion that the electroactive species is neither one of the species in Reaction 7 nor is it in quasi-equilibrium with the species in Reaction 7 on the time scale used here.

Table I shows that there are five other species present in solution: S_2^{2-}, S_3^{2-}, S_5^{2-}, S^{2-} and S_2^-. Because the concentration of the active species must be low and show a strong temperature dependence, only S^{2-} and S_2^- are possible candidates. The concentrations of the polysulfide ions are almost invariant with temperature (25) and even the concentration of S_2^{2-} is too high by an order of magnitude.

Sulfide can be produced from bisulfide according to:

$$HS^- \rightleftarrows H^+ + S^{2-} \tag{8}$$

This is the second dissociation reaction of hydrogen sulfide, with an acidity constant, K_{a2}. Giggenbach (23) gives the temperature dependence of K_{a2} at about 6.5 kcal/mole; this is in accord with acidity constants measured for similar equilibria (32).

Supersulfide can be produced from tetrasulfide:

$$S_4^{2-} \rightleftarrows 2S_2^- \tag{9}$$

with a temperature dependence (21):

$$pK_{eq} = \frac{4533}{T} - 6.42, \quad K_{eq} = \frac{[S_2^-]^2}{[S_4^{2-}]} \tag{10}$$

This "apparent" equilibrium constant is written in terms of concentrations and not activities. This represents a 10.3 kcal/mole activation energy for the temperature dependence of the concentration of supersulfide, which is close to the temperature dependence of the active species concentration found from Figure 4. The line in Figure 4 shows the concentrations of supersulfide predicted by Equation 10. Considering the approximations made in deriving the concentrations from the diffusion parameter, the agreement between Equation 10 and the experimental results is good.

The deviations between Equation 2 and the experimental data can now be understood. At low temperatures, and for the time scales considered here, very little conversion of tetrasulfide to supersulfide takes place (low rate of reaction and thin boundary layers). It is the supersulfide ini-

tially present that determines the response. As the temperature increases the forward rate of Reaction 9 becomes a significant factor. However, at these low overpotentials it is not the sole rate-determining step. Thus the assumption of one rate-determining step used in deriving Equation 2 is not valid here, and deviations between Equation 2 and the experimental data are expected especially at higher temperatures and longer times.

The correct form of the material balances and boundary conditions for an electrode reaction with two rate-determining steps, at least one of which is homogeneous, has been presented in a companion paper (33). Details of the numerical methods used are also given there. Reaction 9 is a dissociation-dimerization reaction, and homogeneous kinetics corresponding to this type of reaction were used in the numerical model. In the general problem four parameters that characterize the system need to be determined. They are W, λ, k_f and k_b. Here we assume that k_f and k_b are related by the equilibrium constant of Equation 10:

$$k_b = \frac{k_f}{K_{eq}} \tag{11}$$

This leaves three parameters to be determined. W and λ were found by a non-linear least squares fit to Equation 2 (14,15). Data at short times were used; as $t \rightarrow 0$, Reaction 9 exerts an increasingly smaller effect on the current response at the electrode. These values of W and λ were used to make the current and time dimensionless.

Assuming equal diffusion coefficients of supersulfide, tetrasulfide and the reaction products, four dimensionless parameters are needed to to calculate a computer-generated dimensionless current vs. time curve: V^*, C_{ob}/C_{rb}, K_{eq}/C_{ob}, and k_f/λ^2. Here species o is supersulfide, and Species r would be one of the species in Reaction 7. Since species r is much higher in concentration than supersulfide C_{ob}/C_{rb} was assumed to be zero. K_{eq}/C_{ob} was calculated from Equation 10, and V^* is determined by the size of the potential step. The forward reaction-rate constant, k_f, was then varied and the computer-generated curves were compared to the experimental curves. Best agreement between the experimental data and the numerical calculations was found when the values of λ were increased slightly from the values obtained from the non-linear least squares fitting of Equation 2. This trend is expected because a smaller value of λ would be obtained by

fitting Equation 2 to data influenced by Reaction 9.

Figures 5 and 6 show samples of the calculated curves from the computer model and the experimental data at 63 and 80 °C. The agreement between the experimental data and computer-generated curves is very good. Table III lists the average values of k_f, k_b and i_o obtained at 63 and 80 C. As mentioned in the results section, the anodic currents were higher than the cathodic currents for a given total overpotential. This leads to higher values of derived exchange current densities for the anodic steps. This is probably related to complexities in the reaction mechanism which are not accounted for by our model (which predicts a symmetrical response).

The values of k_b agree with those observed for other solution-phase dimerization reactions (34). The activation energy for k_f is about 22 kcal/mole which is somewhat smaller than that expected (about 30 kcal/mole) for a solution-phase dissociation reaction (35). However, the uncertainties in the values are about a factor of 2. A change in the value of k_f by less than this amount would give an activation energy close to 30 kcal/mole.

The results presented here are in agreement with trends noted by other investigators. Increasing the sulfur to sulfide ratio (at constant sulfide concentration) lowers both the anodic and cathodic overpotential at redox electrodes (13). Increased efficiency and stability of photoanodes has also been noted (7). In the composition range where these investigations were carried out the predominant polysulfide species are S_3^{2-} and S_4^{2-}. Making the solution more sulfur-rich increases the concentration of tetrasulfide at the expense of trisulfide, which would increase the concentration of supersulfide according to Reaction 9. Decreasing the pH has also been reported to have beneficial effects on photoelectrochemical cell operation (8). In the composition ranges studied this would also have the effect of increasing S_4^{2-} and therefore S_2^-.

The identification of supersulfide as the active species suggests several modifications that could improve the kinetics at a redox electrode in addition to those mentioned above. One way of shifting the equilibrium in Reaction 9 toward supersulfide is to increase temperature. Photoelectrochemical cells are natural candidates for operation at elevated temperatures due to the

large amount of waste heat produced by solar irradiation. While increased concentration of S_2^- would be beneficial there are several disadvantages to increased temperature. The photocorrosion of the semiconductor, which is already a major problem near room temperature, may become a limiting factor at higher temperatures. As temperature increases, the open-circuit potential of liquid-junction photovoltaic cells decreases in a manner similar to that of solid-state photovoltaic cells. Finally, at elevated temperatures the degradation of polysulfides to thiosulfate increases as noted above.

Another way of shifting the equilibrium in Reaction 9 toward the right would be to employ a solvent in which sulfur radical anions are stabilized relative to polysulfide ions. Aprotic, polar solvents such as dimethylformamide (DMF), dimethylsulfoxide (DMSO) and acetone have been shown to stabilize sulfur radicals (36). These solvents are stable over a wide range of potentials. However, the conductivity of these solution is lower than that of aqueous solutions, so higher ohmic losses might be a problem. A good strategy might be to employ the organic as a cosolvent in predominantly aqueous solutions. Results of investigations into mixed aqueous-organic electrolytes will be reported in a subsequent communication.

Conclusions

1. The predominant species in 1M Polysulfide solutions near pH 12 and a sulfur to sulfide ratio of 1 are S_4^{2-} and HS^-.

2. The sulfur radical anion, S_2^-, is the electrochemically-active species at low cathodic and anodic overpotentials.

3. The conversion of tetrasulfide into supersulfide affects the current response at higher temperatures and thicker boundary layers. The kinetic parameters for this reaction are similar to those measured for other dissociation-dimerization reactions.

4. Shifting the equilibrium toward supersulfide should have a beneficial effect on the kinetics and transport processes at the aqueous polysulfide electrode.

Acknowledgement

This work was supported by the Assistant Secretary for Conservation and Renewable Energy, Office of Energy Storage and Distribution of the U.S. Department of Energy under Contract No. DE-AC03-76SF00098.

Nomenclature

Roman

C_{dl}, double layer capacity (F/cm^2)

C_{ob}, C_{rb}; concentrations ($mole/cm^3$)

D_o, D_r, diffusion coefficients (cm^2/sec)

F, Faraday (96,486 C/equiv.)

i_o, exchange current (A/cm^2)

i^*, dimensionless current, $iV^*/W(1+\frac{C_{ob}}{C_r^b})$

K_{a2}, second acidity constant of H_2S

k_b, backward rate constant, Reaction 9 (liter/mole-sec)

K_{eq}, equilibrium constant, Reaction 9 (mole/liter)

k_f, forward rate constant, Reaction 9 (sec^{-1})

n, number of electrons

R, gas constant (J/mole-K)

R_r, linear reaction resistance, $RT/\nu nFi_o$ ($ohm\text{-}cm^2$)

R_s, uncompensated solution resistance ($ohm\text{-}cm^2$)

t, time (sec)

t^*, dimensionless time ($\lambda^2 t$)

t_2, rise time of potential across double layer (sec)

V, total overpotential between working and reference electrode (volts)

V^*, dimensionless potential (nFV/RT)

W, defined by Equation 3 (A/cm^2)

Greek

ν, stoichiometric number

λ, defined by Equation 4 ($sec^{-1/2}$)

References

1. A.B. Ellis, S.W. Kaiser, J.M. Bolts and M.S. Wrighton, *J. Am. Chem. Soc.*, **99,** 2839 (1977).

2. M.A. Russak and C. Creter, *J.Electrochem. Soc.*, **131,** 556 (1984).

3. S. Licht, R. Tenne, G. Dagan, G. Hodes, J. Manassen, D. Cahen, R. Triboulet, J. Rioux and C. Levy-Clement, *Appl. Phys. Lett.*, **46,** 608 (1985).

4. G. Hodes, D. Cahen and M. David, *J. Electrochem. Soc.*, **127,** 2252 (1980).

5. G. Hodes, *Nature*, **285,** 29 (1980).

6. G. Hodes, J. Manassen and D. Cahen, *J. Electrochem. Soc.*, **127,** 544 (1980).

7. D. Lando, J. Manassen, G. Hodes and D. Cahen, *J. Am. Chem. Soc.*, **101,** 3969 (1979).

8. S. Licht and J. Manassen, *J. Electrochem. Soc.*, **132,** 1076 (1985).

9. S. Licht, R. Tenne, H. Flaisher and J. Manassen, *J. Electrochem. Soc.*, **131,** 950 (1984).

10. W.R. Fetzer, *J. Phys. Chem.*, **32,** 1787 (1928).

11. H. Gerischer, *Z. Electrochem.*, **54,** 541 (1950).

12. I.C. Hamilton and R. Woods, *J. Appl. Electrochem.*, **13,** 783 (1983).

13. P.L. Allen and A. Hickling, *Trans. Faraday. Soc.*, **53,** 1626 (1957).

14. Z. Nagy, *Electrochim. Acta*, **25,** 575 (1980).

15. Z. Nagy, *J. Electrochem. Soc.*, **129,** 1943 (1982).

16. G. Schwarzenbach and A. Fischer, *Helv. Chim. Acta.*, **43,** 1365 (1960).

17. A. Teder, *Acta Chemica Scandinavica*, **25,** 1722 (1971).

18. A. Teder, *Ark. Kemi*, **30,** 379 (1969).

19. A. Teder, *Ark. Kemi*, **31,** 173 (1969).

20. W. Giggenbach, *Inorg. Chem.*, **11,** 1201 (1972).

21. W. Giggenbach, *Inorg. Chem.*, **10,** 1306 (1971).

22. S.R. Rao and L.G. Hepler, *Hydrometallurgy*, **3,** 293 (1977).

23. W. Giggenbach, *Inorg. Chem.*, **10,** 1333 (1971).

24. B. Meyer, K. Ward, K. Koshlap and L. Peter, *Inorg. Chem.*, **22,** 2345 (1983).

25. W. Giggenbach, *Inorg. Chem.*, **13,** 1724 (1974).

26. W. Giggenbach, *Inorg. Chem.*, **13,** 1730 (1974).

27. S. Licht, Electrochemical Society Meeting, Las Vegas, Nevada, Paper No. 342, (October 1985).

28. G.P. Power, I.M. Ritchie and M.T. Wylie, *Electrochim. Acta,* **11,** 1633 (1981).

29. R.C. Reid, J.M. Prausnitz and T.K. Sherwood, "The Properties of Gases and Liquids", 3rd Ed., McGraw-Hill, New York, (1977), pp. 590-595.

30. W.M. Latimer, "Oxidation Potentials" , Prentice Hall, New Jersey, (1952).

31. R.J. Remick and E.H. Camara, Lawrence Berkeley Laboratory Report No. LBL-16850 (1983).

32. H.C. Helgeson, *Amer. J. Sci.,* **267,** 729 (1969).

33. P. Lessner, J. Winnick, F.R. McLarnon and E.J. Cairns, Submitted to *J. Electrochem. Soc.* (1986).

34. J.E O'Reilly and P.J. Elving, *J. Am. Chem. Soc.,* **93,** 1871 (1971).

35. K.J. Laidler, "Chemical Kinetics, Second Ed.", McGraw-Hill, New York, (1965), p.200.

36. R.D. Rauh, F.S. Shuker, J.M. Marston and S.B. Brummer, *J. Inorg. Nucl. Chem.,* **39,** 1761 (1977).

Table I: Species Distribution in 1M Na_2S_4, pH=12

Temperature	25 C		63 C		80 C	
Ion	Concentration	% of zero-valent S present	Concentration	% of zero-valent S present	Concentration	% of zero-valent S present
HS^-	0.991 M	———	0.991 M	———	0.991 M	———
S^{2-}	7.9 μM	———	27 μM	———	43 μM	———
S_2^{2-}	0.22 mM	0.02	0.22 mM	0.02	0.22 mM	0.02
S_3^{2-}	0.025 M	5.04	0.025 M	5.04	0.025 M	5.04
S_4^{2-}	0.3 M	89.87	0.3 M	89.85	0.3 M	89.82
S_5^{2-}	0.013 M	5.07	0.013 M	5.07	0.013 M	5.07
S_2^-	22 μM	0.004	0.16 mM	0.024	0.36 mM	0.054

Table II: Selection of Electrocatalyst

Electrocatalyst	Smooth and Reproducible Surface	Corrosion	Takes on Polysulfide Redox Potential	Comments
Cu	Yes	Very Rapid	No	Mixed Potential
Ag	Yes	Rapid	No	Mixed Potential
Mo	Yes	Yes	No	Film on surface
MoS_2	No	No	Yes	Grown by reaction of Mo disk with sulfur at 400 C
Ni	Yes	Yes	Yes	Response changes with time due to visible surface corrosion
NiS	No	No	Yes	Pressed from powder
Co	Yes	No	Yes	No visible chemical corrosion even at elevated temperatures
Pt	Yes	No	Yes	Current response less than that of Co

Table III: Summary of Rate Constants

Temperature	k_f	k_b	i_o
(°C)	(sec^{-1})	(liters/mole-sec)	(mA/cm^2)
< 45	——	——————	1
63	0.025	$\approx 10^5$	1.15 cathodic 1.21 anodic
80	0.15	$\approx 10^5$	2.54 cathodic 2.85 anodic

List of Figures

Figure 1: Equipment Diagram for Potential Step Experiments.

Figure 2: Cell Design.

Figure 3: Current Transients on 0.2 cm^2 Cobalt electrode; x 35.8 °C, □ 63.3 °C, ○ 80.4 °C ;_____ fit to Equation 2.

Figure 4: Active Species Concentration in 1M Na_2S_4 at pH=12; □ calculated from diffusion parameter; _____ calculated from Equation 10.

Figure 5: -10 mV step at 63.4 °C; • experimental data; _____ calculated response with k_f =0.02 sec^{-1}.

Figure 6: -20.1 mV step at 80.4 °C; • experimental data; _____ calculated response with k_f =0.15 sec^{-1}.

APPARATUS BLOCK DIAGRAM

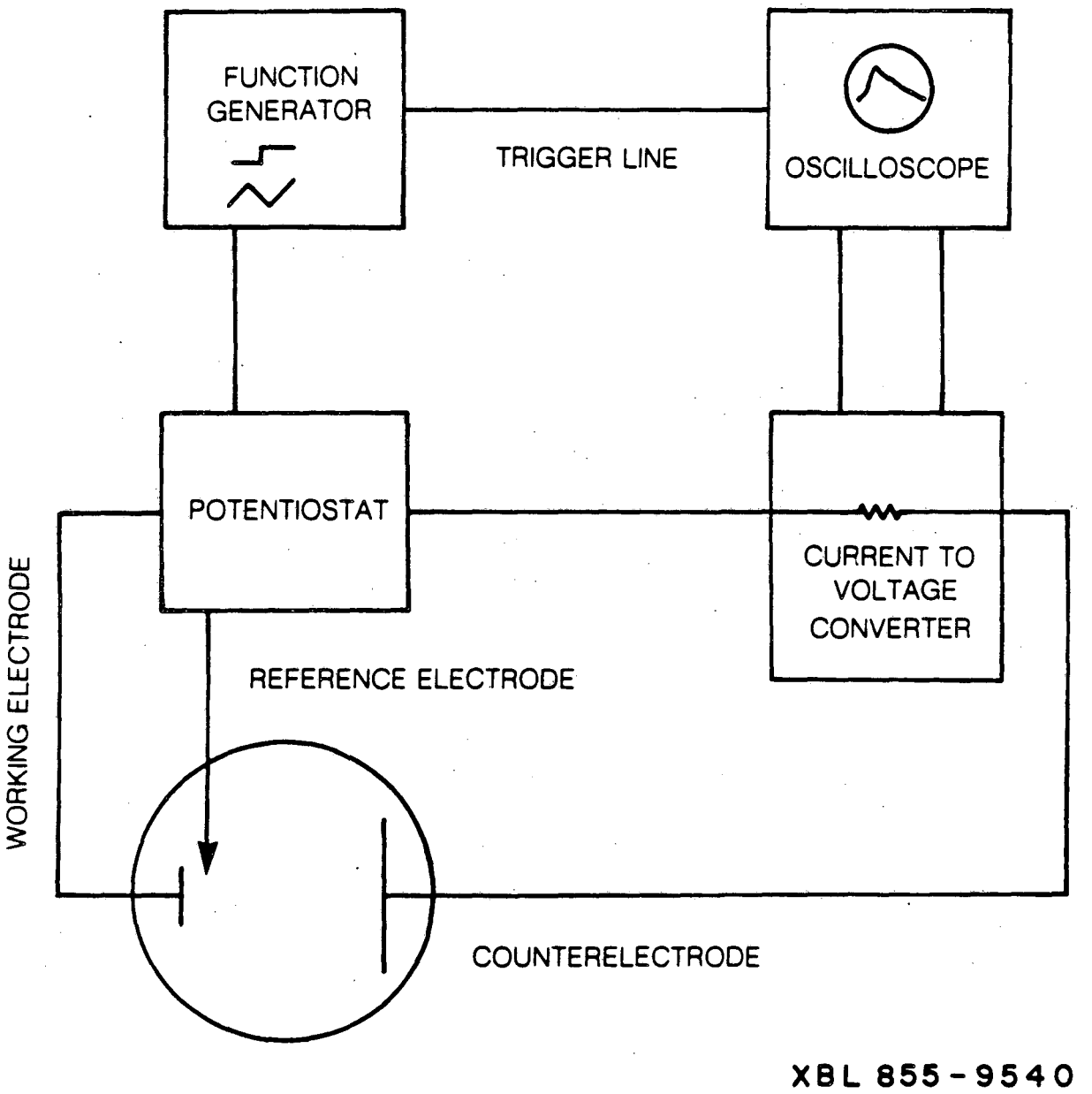

Figure 1

CELL DESIGN

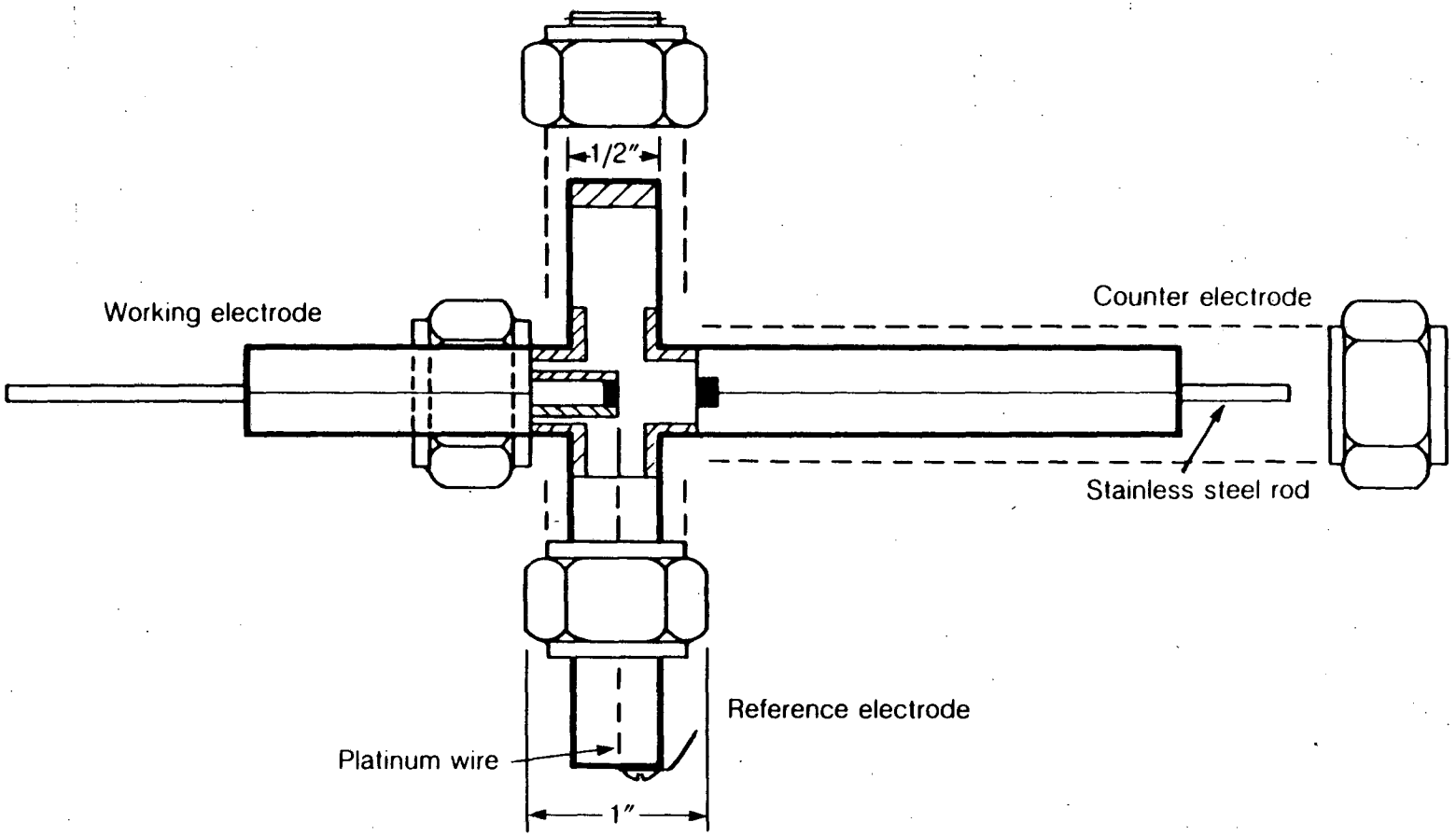

XBL 855-9541

Figure 2

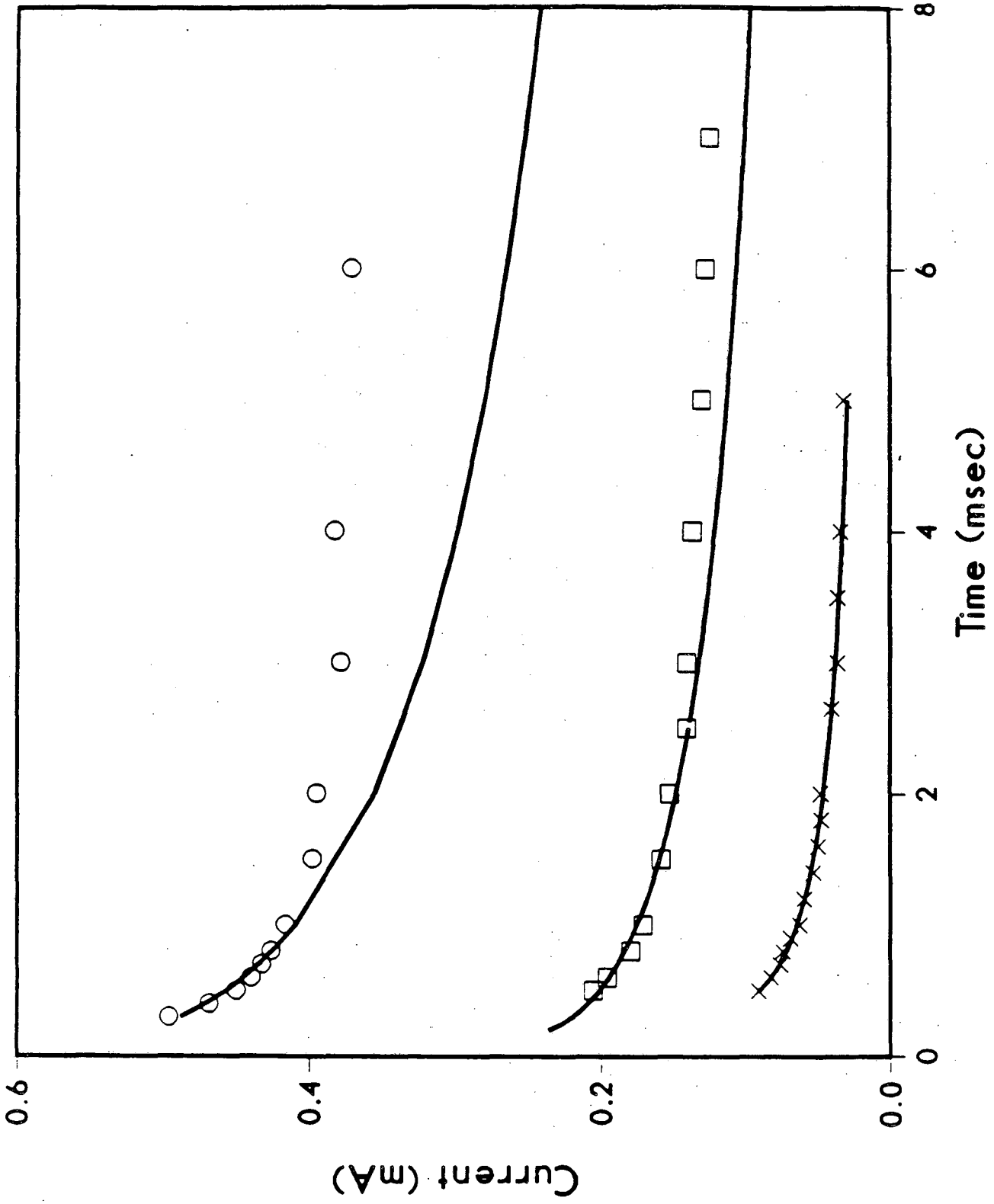

XBL 862-9118

Figure 3

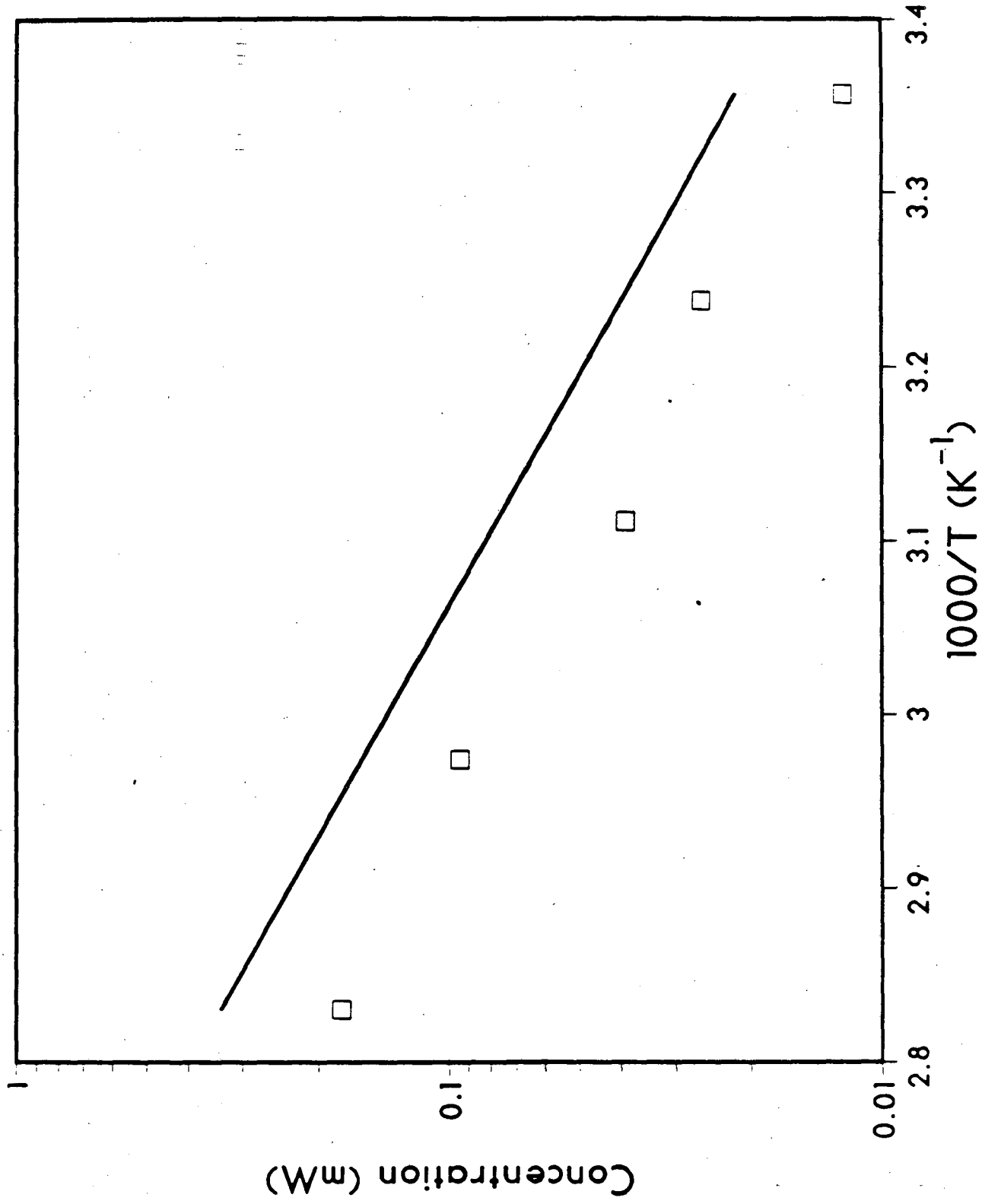

XBL 862-9119

Figure 4

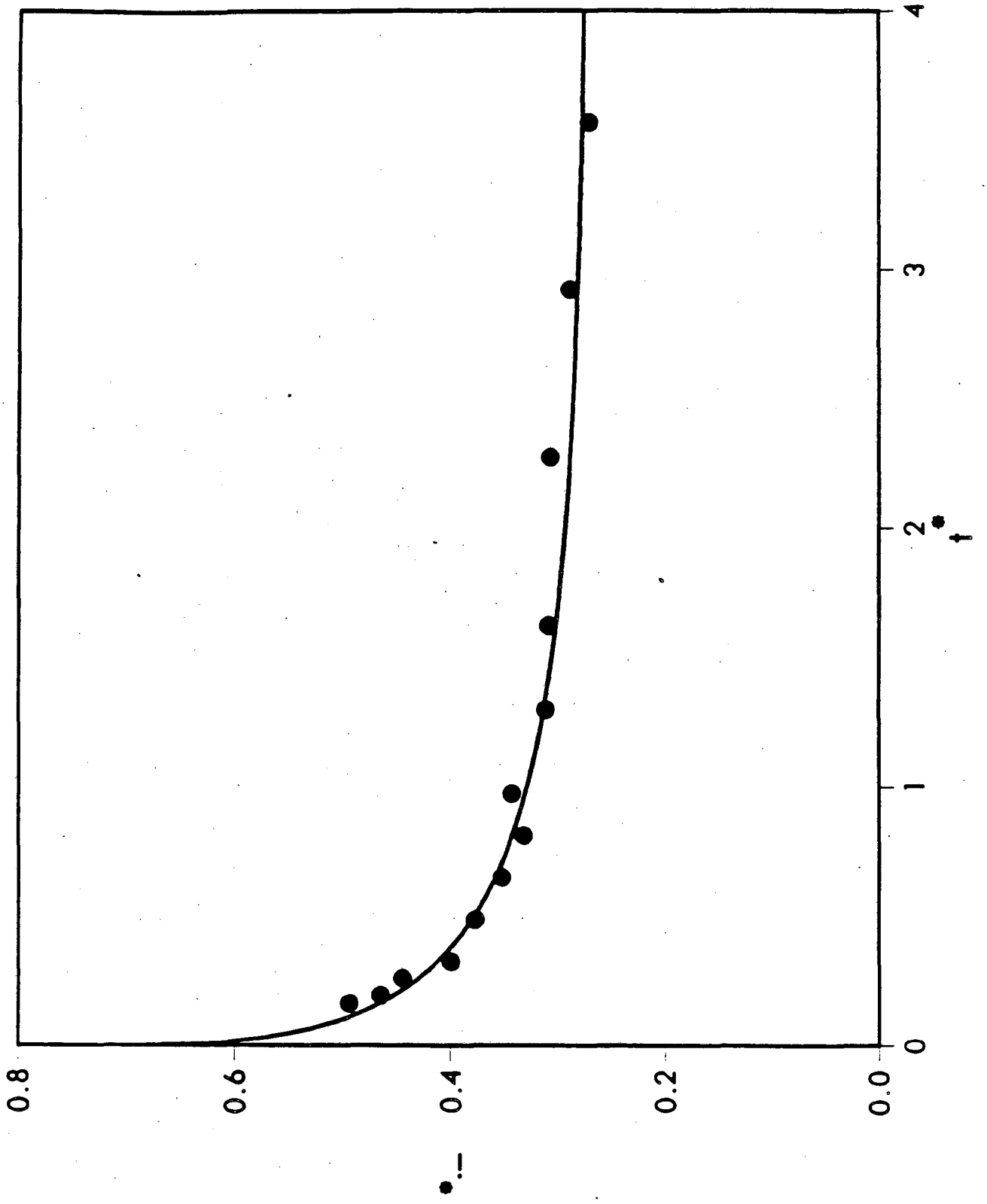

Figure 5

XIII '86-2-9-20

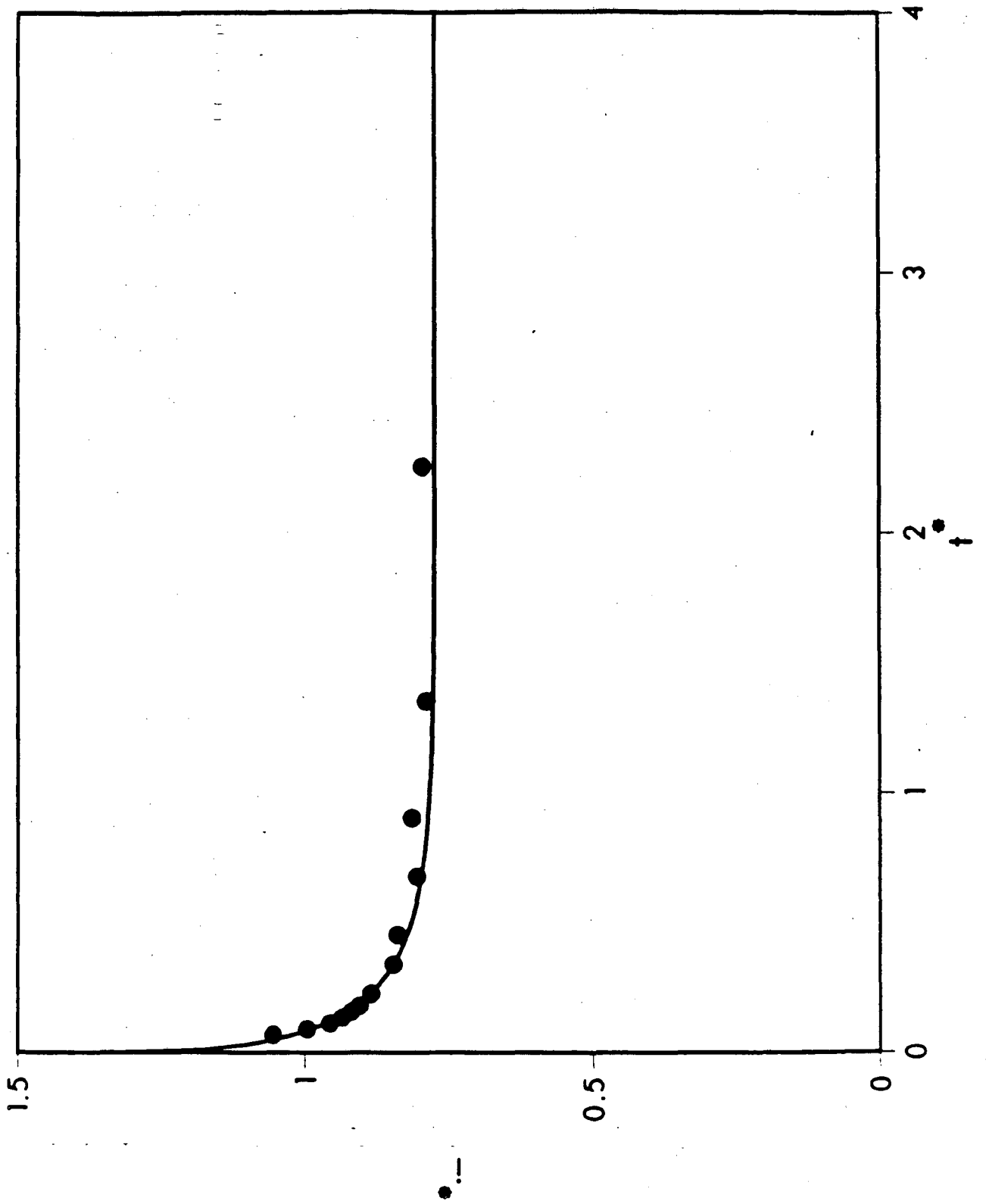

XBL 862-9121

Figure 6

This report was done with support from the Department of Energy. Any conclusions or opinions expressed in this report represent solely those of the author(s) and not necessarily those of The Regents of the University of California, the Lawrence Berkeley Laboratory or the Department of Energy.

Reference to a company or product name does not imply approval or recommendation of the product by the University of California or the U.S. Department of Energy to the exclusion of others that may be suitable.

LAWRENCE BERKELEY LABORATORY
TECHNICAL INFORMATION DEPARTMENT
UNIVERSITY OF CALIFORNIA
BERKELEY, CALIFORNIA 94720